JCTC Journal of Chemical Theory and Computation

Article

pubs.acs.org/JCTC

Density Matrix Embedding: A Strong-Coupling Quantum Embedding Theory

Gerald Knizia* and Garnet Kin-Lic Chan

Department of Chemistry, Princeton University, Princeton, New Jersey 08544, United States

ABSTRACT: We extend our density matrix embedding theory (DMET) [*Phys. Rev. Lett.* **2012**, *109*, 186404] from lattice models to the full chemical Hamiltonian. DMET allows the many-body embedding of arbitrary fragments of a quantum system, even when such fragments are open systems and strongly coupled to their environment (e.g., by covalent bonds). In DMET, empirical approaches to strong coupling, such as link atoms or boundary regions, are replaced by a small, rigorous quantum bath designed to reproduce the entanglement between a fragment and its environment. We describe the theory and demonstrate its feasibility in strongly correlated hydrogen ring and grid models; these are not only beyond the scope of traditional embeddings but even challenge conventional quantum chemistry methods themselves. We find that DMET correctly describes the notoriously difficult symmetric dissociation of a 4 × 3 hydrogen atom grid, even when the treated fragments are as small as single hydrogen atoms. We expect that DMET will open up new ways of treating complex strongly coupled, strongly correlated systems in terms of their individual fragments.

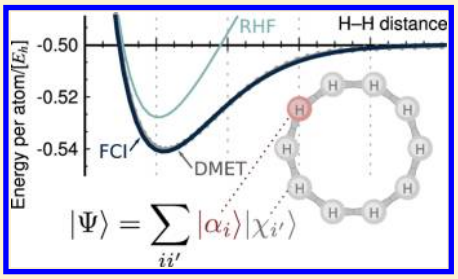

Embedding techniques are powerful tools for enabling high-level many-body treatments on system sizes they cannot normally reach. They work by dividing a chemical system into fragments, each of which is handled individually; the interaction with the other fragments—the environment—is treated in a simplified way. In this article, we are concerned with embeddings for fragments which are *strongly* coupled to their environment, for example via covalent bonds.

A particular embedding is characterized by the precise manner in which the environment and its influence on the fragment are represented. To date, most embedding techniques represent the environment through a one-particle embedding potential v. For example, in QM/MM methods, v is obtained through electrostatics or polarization interactions,[1,2] while in *ab initio* DFT embedding, v is the derivative of the nonadditive energy functional.[3−6] However, an embedding potential, regardless of how it is obtained, cannot represent the effect of the environment on the many-body fragment state when the coupling is *strong*.[7] This is illustrated by the simple example of embedding a hydrogen atom A within a hydrogen molecule AB. If hydrogen atom B is represented by an embedding potential v, then hydrogen atom A appears as a closed system with a single electron; thus, any wave function description of the fragment, regardless of the choice of v, provides no information on electron correlation.

This failure of potential based embedding is rooted in the fact that the fragments are *open* systems that are entangled with their environment. Is it possible *even in principle* to formulate an embedding description of an open fragment? This question has far reaching consequences; an affirmative answer would imply, for example, that one could in principle exactly calculate the properties of a bulk diamond crystal by treating a single embedded carbon atom. Here, we argue that this is indeed the case. The key is to represent the environment not by a potential but rather through a quantum *bath* that reproduces the entanglement of the embedded fragment with the full environment. In existing embedding approaches, empirical link atoms or boundary regions[8] can be thought of as baths, but here we show that an *exact* bath, that exactly reproduces *all* many-body environment effects, can in fact be defined. In realistic systems, the construction of this exact bath is not practical. However, as we show below, this point of view naturally leads to a practical embedding method which we call *density matrix embedding theory* (DMET).

We have previously introduced DMET in the context of fermionic lattice models[9] where it showed excellent performance, in particular, in comparison to the more complex dynamical mean-field theory (DMFT). Here, we describe the extension and modification of DMET to treat inhomogeneous systems and the full chemical Hamiltonian with long-range interactions. We note especially that DMET is defined through simple linear algebra and avoids the numerical issues of inverse problems associated with constructing potential embeddings, as found in *ab initio* DFT embedding (see also ref 10 for a different solution to the inverse problem).

We use the following notation: The full quantum system Q is spanned by an orthogonal one-particle basis (e.g., an symmetrically orthogonalized atomic orbital basis). The orthogonal basis functions are indexed by r, s ,t, and u and referred to as *sites*. We write the Hamiltonian as[11]

$$H = \sum_{rs} h_s^r E_r^s + \frac{1}{2} \sum_{rstu} V_{tu}^{rs} E_{rs}^{tu} \tag{1}$$

Received: November 28, 2012
Published: February 21, 2013

where E^s_r and E^{tu}_{rs} are spin-summed excitation operators, e.g., $E^s_r = \sum_\sigma a^\dagger_{s\sigma} a_{r\sigma}$,[11] and $h^r_s = \langle r|v_{\mathrm{nuc}} - (1/2)\Delta|s\rangle$ and $V^{rs}_{tu} = \langle rs|r^{-1}|tu\rangle$ are spatial matrix elements over the core Hamiltonian and Coulomb operators, respectively. Q is divided into sets of sites called *fragments*, such that each site occurs in exactly one fragment. Fragments are handled sequentially, and for each fragment A, the union of the other fragments is treated as environment B. $|A|$ is the number of sites in set A.

First, let us review the exact formal bath that exactly embeds a given fragment A. Let Q be the full quantum system and $|\Psi\rangle$ be an eigenstate of Q. $|\Psi\rangle$ may expanded as

$$|\Psi\rangle = \sum_{ij} \psi_{ij} |\alpha_i\rangle |\beta_j\rangle \tag{2}$$

where $|\alpha_i\rangle$ and $|\beta_i\rangle$ are states in the Fock space spanned by the fragment A and the environment B, respectively. Simple algebra shows that

$$\begin{aligned} |\Psi\rangle &= \sum_{ij} \psi_{ij} |\alpha_i\rangle |\beta_j\rangle \\ &= \sum_i |\alpha_i\rangle \left(\sum_j \psi_{ij} |\beta_j\rangle \right) \\ &= \sum_i |\alpha_i\rangle |\tilde{\chi}_i\rangle \\ &= \sum_{ii'} \psi_{ii'} |\alpha_i\rangle |\chi_{i'}\rangle \end{aligned} \tag{3}$$

where $|\tilde{\chi}_i\rangle = \sum_j \psi_{ij} |\beta_j\rangle$ and $|\chi_i\rangle$ is the orthogonalized set of $|\tilde{\chi}_i\rangle$ states. (This rewriting is closely related to the Schmidt decomposition of quantum information theory[12]). Note that in the last line, although $|\chi_{i'}\rangle$ are states in the environment B, there are only M_A of them: the dimension of the Fock space of A. This set of special environment states defines the bath. We see that (i) no matter how large the environment, in a given state $|\Psi\rangle$, a fragment A can only be entangled with M_A environment states in B. Thus the entanglement effect of the environment is *fully represented by a bath of the same size as the fragment* it is embedding. This combination of the fragment with its bath we refer to as the *embedded* system. (ii) If $|\Psi\rangle$ is an eigenfunction of a Hamiltonian H (that acts in the full system Q), it is also an eigenfunction of a projected Hamiltonian defined in only the embedded system, $H' = PHP$, where

$$P = \sum_{ii'} |\alpha_i\rangle |\chi_{i'}\rangle \langle \alpha_i| \langle \chi_{i'}| \tag{4}$$

H' is the embedding Hamiltonian.

We thus have established that fragments can, in principle, always be exactly embedded by baths no larger than the fragments themselves. While exact, this result is purely formal, because to construct the bath states $\{|\chi_i\rangle\}$ we require knowledge of the state $|\Psi\rangle$ of the full system Q. However, it naturally suggests a practical approximation: construct the bath from an approximate state of Q, $|\Phi\rangle$, and use this approximate bath in a subsequent high-level treatment of the embedded fragments. This is the combination we aim for in DMET.

A simple choice for $|\Phi\rangle$ is a Slater determinant (for example, as obtained from a mean-field treatment of the full system). For a Slater determinant, the associated bath and embedding Hamiltonian are particularly simple: they can be obtained from single-particle linear-algebra rather than the many-particle decomposition in eq 3, as we now show. First note that, for any $|\Psi\rangle$, the fragment many-body states $|\alpha_i\rangle$ in eq 3 live in the Fock space spanned by the one-particle fragment sites $\mathcal{F}(|i\rangle)$, $i \in A$. In the special case where $|\Psi\rangle = |\Phi\rangle$ is a determinant, also the bath states $|\chi_i\rangle$ live in a Fock space defined by one-particle bath orbitals $\{|b\rangle\}$ (at most $|A|$), multiplied by a common core determinant. This is seen as follows. Let $|p\rangle = \sum_r C^r_p |r\rangle$ denote the N occupied orbitals of $|\Phi\rangle$, where $p = 1...N$, $r \in Q$. Let

$$S_{pq} = \sum_{i \in A} \langle p|i\rangle \langle i|q\rangle \tag{5}$$

define the overlap matrix S of the orbitals *projected onto the sites of fragment A*. Then the eigenvectors of S define a rotation of the occupied orbitals $|p\rangle \rightarrow |\tilde{p}\rangle$ which divides them into two sets: a set of $N - |A|$ occupied orbitals with zero eigenvalues, and thus *without* any component on the fragment sites, and a set of $|A|$ occupied orbitals with nonzero eigenvalues, which have overlap with the fragment sites. We call the former "pure environment orbitals" and the latter "entangled orbitals." Projecting the entangled orbitals $\tilde{p} = 1...|A|$ onto the environment sites B, and normalizing, then yields a set of bath orbitals $|b\rangle$ of the same number as fragment sites

$$\{|b\rangle\} = \left\{ \frac{\sum_{j \in B} |j\rangle \langle j|\tilde{p}\rangle}{\| \sum_{j \in B} |j\rangle \langle j|\tilde{p}\rangle \|}; \tilde{p} = 1...|A| \right\} \tag{6}$$

Rewriting $|\Phi\rangle$ in terms of the rotated orbitals $|\tilde{p}\rangle$, and expressing each $|\tilde{p}\rangle$ in terms of its fragment, bath, and pure environment components, we see that the many-body bath states $|\chi_i\rangle$ span the same space as $\mathcal{F}(|b\rangle) \otimes \det(e_1 e_2 ... e_{N-|A|})$, where $\det(e_1 e_2 ... e_{N-|A|})$ is the determinant of pure environment orbitals. In other words, when split across a fragment and environment, a determinant $|\Phi\rangle$ appears as a CAS-CI (complete active space configuration interaction) expansion in a half-filled active *embedding* basis of fragment plus bath orbitals, $\{|i\rangle\} \oplus \{|b\rangle\}$, with a core determinant of pure environment orbitals $|e\rangle$; the total number of electrons in the active space is $|A|$.

We next construct the embedding Hamiltonian corresponding to the Slater determinant $|\Phi\rangle$. Formally, this is defined from the many-body projection eq 4, but for the case of a Slater determinant, it can be constructed by a simple change of single-particle basis. We define the embedded Hamiltonian H' by projecting H into the space $\mathcal{F}(|i\rangle) \otimes \mathcal{F}(|b\rangle) \otimes \det(e_1 e_2 ... e_{N-|A|})$. This is equivalent to transforming H into the active space of the embedding basis (fragment plus bath orbitals) and including a core contribution from the pure environment determinant, $\det(e_1 e_2 ... e_{N-|A|})$. Denoting the embedding basis by labels v, w, x, and y and its representation in terms of the full system sites by $|x\rangle = B^r_x |r\rangle$ (i.e., x runs over i and b, and B^r_x is the orbital coefficient matrix with $B^r_x = \delta^r_i$ and with B^r_b as obtained by eq 6), we find

$$H' = \sum_{vw} h^v_w E^w_v + \frac{1}{2} \sum_{vwxy} V^{vw}_{xy} E^{xy}_{vw} \tag{7}$$

$$h^v_w = B^r_v h^r_s B^s_w + f^{\mathrm{core}}_{vw} \tag{8}$$

$$V^{vw}_{xy} = B^r_v B^w_s V^{rs}_{tu} B^t_x B^u_y \tag{9}$$

If the full system $|\Phi\rangle$ was obtained from a Hartree−Fock calculation, then carrying out a Hartree−Fock calculation in this embedded system with the embedding Hamiltonian H'

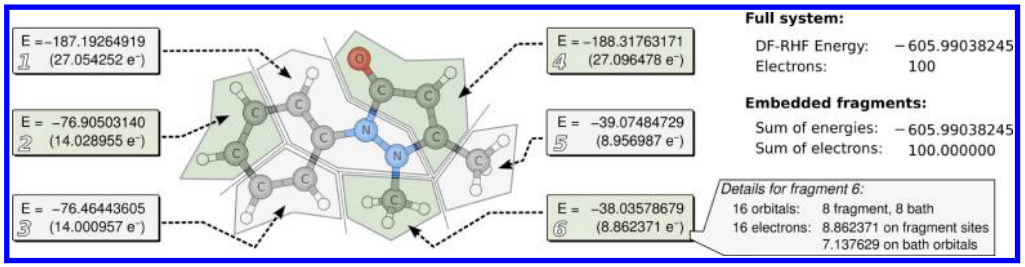

Figure 1. Example for HF in HF embedding: A molecule is split into random atomic fragments. For each fragment, an embedding is constructed, and the embedded system is treated with Hartree−Fock. The left panel shows the obtained distribution of energy and electrons among the fragments. The right inset shows how the open system embedding (e.g., a fractional electron number) is realized by coupling to a bath.

yields a mean-field Fock operator f' for which $|\Phi\rangle$ is an eigenstate.

In Figure 1, we numerically demonstrate the exactness of the above mean-field embedding by the following process: (i) A Hartree−Fock calculation is performed on a molecule. (ii) The molecule is split into arbitrary groups of atoms as fragments. For each fragment, an embedding is constructed (bath orbitals and H') and a Hartree−Fock calculation is run on the embedded system. (iii) The system is reassembled by adding up the energies and electrons located on the various fragments. We note that only the electrons and energy contributions associated with the fragment sites should be considered when reassembling the system, not the contributions associated exclusively with bath or pure environment orbitals, as this would lead to double counting. To that end, we define the energy of a fragment A using the one- and two-particle density matrices, γ and Γ, with at least one index in fragment A

$$E_A = \sum_{i\in A,s} \gamma_s^i h_i^s + \frac{1}{2} \sum_{i\in A,stu} \Gamma_{tu}^{is} V_{is}^{tu} \tag{10}$$

Note that γ and Γ include the contributions from the pure environment orbitals (the core determinant). Note also that generalizations of eq 10 can be used to calculate other expectation values of the fragmented system, despite the fact that there is no wave function for all fragments combined. As we see from Figure 1, the embedding allows an arbitrary fragmentation into open fragments to be exactly reassembled (note the fractional electron numbers!), recovering the exact Hartree−Fock energy of the wave function $|\Phi\rangle$ used to contruct it.

We now return to the DMET. Recall that here we still construct the embedding based on a mean-field $|\Phi\rangle$ of the full system Q but use it to embed high level calculations on the fragments rather than Hartree−Fock. For each fragment A, the high level calculation on the embedded system (fragment sites, bath orbitals, and Hamiltonian H') yields a correlated $|\Psi_A\rangle$.

The high level calculation is a correlated calculation in the "active" embedding space $\mathcal{F}(|i\rangle) \otimes \mathcal{F}(|b\rangle)$ in the presence of a frozen pure environment determinant $\det(e_1e_2...e_{N-|A|})$. However, to ensure a consistent fragment description by the mean-field $|\Phi\rangle$ and the high-level embedded $|\Psi_A\rangle$, we require an additional self-consistency cycle, described below. Note that the fragment's total wave function $|\Psi_A\rangle$ is $\det(e_1e_2...e_{N-|A|})$ multiplied by the embedding space part, and this wave function should have the correct symmetry and electron number for the whole system Q (which are input quantities). Since we know $\det(e_1e_2...e_{N-|A|})$ and the target quantum numbers of $|\Psi_A\rangle$, the quantum numbers in the embedding space directly follow.

To ensure self-consistency between the correlated and high-level fragment descriptions, we require a self-consistency condition. The choice is not unique, but we note that a mean-field state is characterized by its one-particle density matrix $\langle\Phi|a_r^\dagger a_s|\Phi\rangle$, and thus it is convenient to enforce consistency at the level of the density matrices by minimizing the metric

$$\Delta = \sum_A \sum_{rs\in A} \|\langle\Phi|a_r^\dagger a_s|\Phi\rangle - \langle\Psi_A|a_r^\dagger a_s|\Psi_A\rangle\|^2 \tag{11}$$

Here, we define the density matrix difference only over (intra)fragment sites for simplicity, but very similar results are obtained by defining the difference over fragment plus bath sites for each embedding, as we did in our earlier work.[9] $|\Phi\rangle$ is then obtained from a mean-field Fock operator f augmented by a set of one-particle operators u_A for each fragment, with $u_{rs}^u = 0$ for $r \notin A$ or $s \notin A$. The u_A's are chosen to minimize Δ and capture the correlation effects on the one-particle density matrix. The embedded Hamiltonian is also augmented with the correlation operators on the fragments other than the one currently being considered, projected into the embedding basis. [u_A is omitted for H_A of fragment A because the embedded system includes all degrees of freedom and the exact Hamiltonian for $\mathcal{F}(|i\rangle)$, $i \in A$. The correlation effect on the $i \in A$ sites is thus already accounted for by the real Hamiltonian, and including the one-particle correlation operator u_A additionally would cause double counting.] The DMET self-consistency cycle is thus:

(1) The full system is treated at the Hartree−Fock level using the Fock operator $f + \sum_A u_A$ to determine $|\Phi\rangle$. Initially all u_A's are zero.

(2) For each fragment, $|\Phi\rangle$ is used to construct an embedding basis. The embedding Hamiltonian for fragment A, $H_{A'}$, is obtained by projecting $H + \Sigma_{A'\neq A} u_{A'}$ into the embedding basis following eq 7 . The embedded fragment's state $|\Psi_A\rangle$ is calculated at a correlated level, for example, with full configuration interaction (FCI).

(3) For each fragment A, we adjust the correlation operator $u_A = \sum_{rs\in A} u_{rs}^A E_r^s$ to minimize the difference between the Hartree−Fock one-particle density matrix and the correlated one-particle density matrix, $\Delta_A = \sum_{rs\in A} \|\langle\Phi|a_r^\dagger a_s|\Phi\rangle - \langle\Psi_A|a_r^\dagger a_s|\Psi_A\rangle\|^2$. [Note that $\langle\Phi|$ and $|\Psi_A\rangle$ can differ only in the embedded system, both carrying the same pure environment core determinant when viewed as wave functions for the full system.]

(4) The cycle is iterated until all u_{rs}^A converge.

In our trial systems the metric eq 11 could always be fitted exactly (i.e., at convergence, Δ is numerically zero; note that

with this metric we have as many variables $[u^A_{rs}]$ as data points $[\langle a^\dagger_r a_s\rangle; r,s \in A]$). [It was pointed out to us that at convergence the self-consistency cycle does not necessarily minimize the metric.[13] If the metric can be fitted exactly, this does not occur.] As a result, the one-particle density matrix elements $\langle a^\dagger_r a_s\rangle; r,s \in A$ from the embedded correlated wave function (for fragment A) and the full system mean-field wave function (common to all fragments) *exactly* agree at convergence. It further guarantees that the correlated total electron number summed over all fragments $\sum_A \sum_{r\in A} \langle \Psi_A | a^\dagger_r a_r | \Psi_A \rangle$ is the correct integer, since it is the same as in $|\Phi\rangle$, $\sum_r \langle \Phi | a^\dagger_r a_r | \Phi \rangle$. The fitting metric we used previously involving both fragment and bath orbitals[9] did not have this property but can be easier to converge in the presence of strong correlations.

In order to test whether the DMET provides reasonable results, we now consider simple model systems exhibiting strong correlation, namely, hydrogen rings, chains, and grids. Such systems have recently emerged as a rich testbed for new correlation methods, as the strength of the correlation can be readily tuned from weak to strong by changing the hydrogen atom spacing.[14−20] Note that such systems show high degeneracy and are difficult to handle even with full correlation treatments. Furthermore, as we argued in the introduction, any choice of fragment will be strongly coupled to the rest of the system, so potential based embeddings cannot possibly describe them. All calculations employ a minimal hydrogen basis consisting of orthogonalized 1s-like AO functions obtained from an underlying cc-pVTZ basis, except for the H_{50} calculation, for which we use a STO-6G basis to retain compatibility with earlier references. For the high level treatment of the embedded systems, we use FCI. All calculations are spin-adapted, and both the mean-field (restricted HF) and correlated (FCI) calculations use singlet wave functions. As the DMET self-consistency metric we used eq 11, except for the three-site calculation on the 4 × 3 grid, where the previous metric[9] was used to avoid convergence problems at $r > 3.8a_{bohr}$. The source code for the prototype program will be made available online.[21]

As the simplest nontrivial example, we investigate the symmetric dissociation of a ring of 10 hydrogen atoms (that is, all bonds are simultaneously stretched). The system is fragmented into individual 1s orbitals of the hydrogen atoms, and thus each site is one fragment. The results are shown in Figure 2. The one-site DMET calculation almost exactly reproduces the reference FCI curve. Note that each correlated fragment calculation corresponds to a FCI calculation on only two orbitals, the H 1s orbital and a single bath orbital, and is thus a trivial 3 × 3 matrix diagonalization. [Two orbitals span four two-electron states, of which three are singlet.]

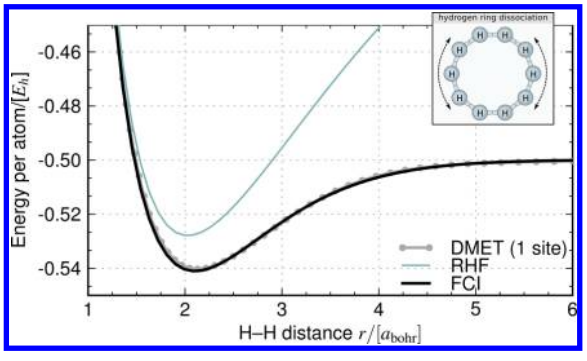

Figure 2. Symmetric stretching of a H_{10} ring: Shown are the exact results (FCI), the mean-field results (RHF), and the one-site DMET results. In one-site DMET, the system is fragmented into individual atoms treated with FCI, and embeddings are constructed from full system RHF.

As a second example, we choose an inhomogeneous system: the linear H_{50} chain (Figure 3). FCI on this system would require on the order of 10^{28} determinants, so truly exact results cannot be calculated. However, near-exact reference data can be obtained by the quantum chemistry density matrix renormalization group (DMRG).[22] We here take the data from Hachmann et al.[23] This particular system has also been the subject of a recent DMFT study by Lin et al.,[19] the results of which are shown for comparison. It is clear that the one-site DMET once again closely reproduces the reference values. Again the fragment calculations are two orbital FCI and thus numerically trivial. It is noteworthy that in this case DMET does better than the more complex DMFT, likely due to its ability to treat long-range interactions with the bath beyond mean-field.

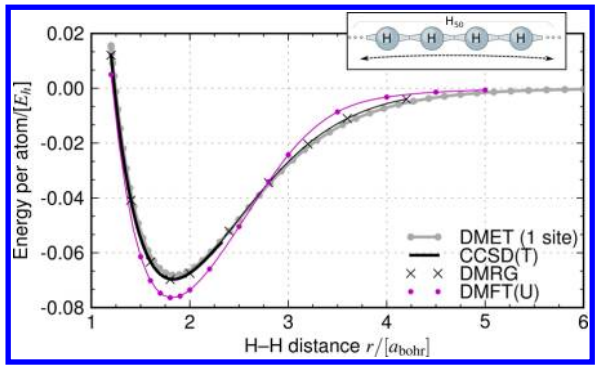

Figure 3. Symmetric stretching of a H_{50} chain. Shown are reference DMRG[23] and CCSD(T) data, the mean-field results (RHF), the one-site DMET results, and the DMFT results by Lin et al.[19] Energies are plotted against the STO-6G dissociation limit of −0.471 040 E_h per atom.

For a more challenging system, we now turn to a two-dimensional inhomogeneous system, the 4 × 3 hydrogen grid. This system is very pathological—it is nonbinding at the Hartree−Fock level, and converging the normally *very* robust FCI[24] required hundreds of iterations for some points. As shown in Figure 4, even here the one-site DMET qualitatively

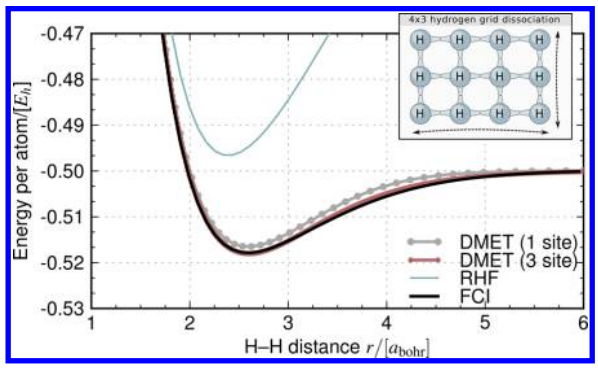

Figure 4. Symmetric stretching of a 4 × 3 hydrogen grid. In the three-site DMET, the system is fragmented into four columns of three hydrogens each.

reproduces the FCI binding curve. The calculations remain as trivial to perform as for the one-dimensional systems. Additionally, if we embed entire columns of atoms, carrying out a three-site DMET, the agreement between the embedded and the reference results becomes almost perfect.

The accuracy of these results may seem surprising, given that the systems are strongly correlated but the embedding is obtained from an uncorrelated, qualitatively incorrect, mean-field $|\Phi\rangle$. However, it is only the bath *states* that are determined from the mean-field theory. Once those states are determined, the embedded Hamiltonian is constructed exactly, and the coupling between the fragment sites and the bath orbitals is obtained by FCI, not mean-field. This allows the fragment state to correctly transition from the delocalized regime of weak correlation to the entangled spin regime of strong correlation. As long as the entanglement is reasonably local and does not involve the *pure* environment orbitals, we can expect good results.

The robustness and simplicity of DMET, even in the presence of strong coupling and strong correlation, makes it unique among current embedding approaches and suggest that it could be useful in a wide range of applications. The next step will be to apply the theory to more realistic and larger scale chemical problems. We are now pursuing these studies.

AUTHOR INFORMATION

Corresponding Author

*E-mail: knizia@princeton.edu.

Notes

The authors declare no competing financial interest.

ACKNOWLEDGMENTS

This work was supported by the Department of Energy, Office of Science, through Grant No. DE-FG02−-07ER46432 and the Computational Materials Science Network (DE-SC0006613).

REFERENCES

(1) Lin, H.; Truhlar, D. *Theor. Chem. Acc.* **2007**, *117*, 185−199.
(2) Senn, H. M.; Thiel, W. *Angew. Chem., Int. Ed.* **2009**, *48*, 1198−1229.
(3) Cortona, P. *Phys. Rev. B* **1991**, *44*, 8454−8458.
(4) Wesolowski, T. A.; Warshel, A. *J. Phys. Chem.* **1993**, *97*, 8050−8053.
(5) Huang, C.; Pavone, M.; Carter, E. A. *J. Chem. Phys.* **2011**, *134*, 154110.
(6) Goodpaster, J. D.; Ananth, N.; Manby, F. R.; Miller, I. T. F. *J. Chem. Phys.* **2010**, *133*, 084103.
(7) Note, we are careful to write "many-body" fragment state. A potential *is* formally sufficient to represent the effect of the environment on the single-particle *density*, and this is the basis of exact DFT embedding. However, we assume here that we wish to describe the fragment with a high-level *many-body* treatment, not only at the level of the density. In this case, the environment cannot be represented by a potential.
(8) Slavíček, P.; Martínez, T. J. *J. Chem. Phys.* **2006**, *124*, 084107 provides an overview over such techniques.
(9) Knizia, G.; Chan, G. K.-L. *Phys. Rev. Lett.* **2012**, *109*, 186404.
(10) Manby, F. R.; Stella, M.; Goodpaster, J. D.; Miller, T. F. *J. Chem. Theory Comput.* **2012**, *8*, 2564−2568.
(11) Kutzelnigg, W. *J. Chem. Phys.* **1982**, *77*, 3081.
(12) Peschel, I. *Braz. J. Phys.* **2012**, *42*, 267−291.
(13) Tsuchimochi, T.; Voorhis, T. V. Private communication.
(14) Tsuchimochi, T.; Scuseria, G. E. *J. Chem. Phys.* **2009**, *131*, 121102.
(15) Mitrushchenkov, A. O.; Fano, G.; Linguerri, R.; Palmieri, P. *Int. J. Quantum Chem.* **2012**, *112*, 1606−1619.
(16) Stella, L.; Attaccalite, C.; Sorella, S.; Rubio, A. *Phys. Rev. B* **2011**, *84*, 245117.
(17) Al-Saidi, W. A.; Zhang, S.; Krakauer, H. *J. Chem. Phys.* **2007**, *127*, 144101.
(18) Bytautas, L.; Henderson, T. M.; Jiménez-Hoyos, C. A.; Ellis, J. K.; Scuseria, G. E. *J. Chem. Phys.* **2011**, *135*, 044119.
(19) Lin, N.; Marianetti, C. A.; Millis, A. J.; Reichman, D. R. *Phys. Rev. Lett.* **2011**, *106*, 096402.
(20) Sinitskiy, A. V.; Greenman, L.; Mazziotti, D. A. *J. Chem. Phys.* **2010**, *133*, 014104.
(21) The source code of the prototype DMET program will be made available at http://www.princeton.edu/chemistry/chan/dmet_chm/.
(22) Chan, G. K.-L.; Sharma, S. *Annu. Rev. Phys. Chem.* **2011**, *62*, 465−481.
(23) Hachmann, J.; Cardoen, W.; Chan, G. K.-L. *J. Chem. Phys.* **2006**, *125*, 144101.
(24) Knowles, P.; Handy, N. *Chem. Phys. Lett.* **1984**, *111*, 315−321.